Probing the polarity of GABAergic transmission in vivo

Olivier Dubanet[1], Arnaldo Ferreira[1], Andreas Frick[1], Hajime Hirase[2], Anna Beyeler[1], Xavier Leinekugel[1]*

1. University of Bordeaux, INSERM U1215, Neurocentre Magendie, 33077 Bordeaux, France

2. Center for Translational Neuromedicine, University of Copenhagen

*corresponding author : xavier@arcadi.eu

Abstract

In vitro studies have reported high intracellular chloride levels, depolarizing and potentially excitatory actions of GABA in various pathological conditions. Consequently, great expectations are now pinned on drugs potentially restoring low $[Cl^-]i$ as novel therapies for a wide range of brain disorders. However, the clinical relevance of this hypothesis remains largely speculative because of the yet unresolved technical difficulty to evaluate the polarity of GABAergic transmission in vivo. Here, we show that the polarity of GABAergic transmission can be probed across the CA3 hippocampal circuit in vivo with single cell resolution, by combining extracellular detection of unitary inhibitory postsynaptic field-potentials (fIPSPs) and silicon probe recording of the firing activity of multiple individually identified neurons. As an example application, we provide direct evidence for depolarizing actions of perisomatic GABAergic transmission and time-locked excitation of CA3 pyramidal neurons in acute and chronic mouse models of epilepsy.

Introduction

GABAergic inhibition relies on ionotropic GABA-A and metabotropic GABA-B receptors. The fast and time-locked inhibition considered essential for neuronal coding is the one mediated by GABA-A receptors (GABA-A R), permeable to chloride ions (Cl^-). In normal conditions, neurons maintain a low intracellular concentration of chloride ($[Cl^-]i$), so that the reversal potential of Cl^- mediated currents is more negative than the resting potential[1]. GABA release therefore generates an influx of Cl^-, with an hyperpolarizing effect on membrane potential, and inhibition of neuronal discharge.

Recent publications have proposed the implication of defective inhibition in the etiology of various pathologies including epilepsy, depression, schizophrenia, Down Syndrome or Autism Spectrum Disorders [2-9]. In vitro experiments have suggested that defective function of the K-Cl co-transporter KCC2, that would normally extrude Cl^- from the cell, was responsible for a reversed polarity of GABAergic synaptic transmission from inhibitory to excitatory, participating in epileptogenesis in animal models [10-17] as well as in human tissue resected from epileptic patients [18-20]. But one major difficulty in the study of GABAergic inhibition is to avoid artefactual interference with the native Cl^- gradient, a main determinant of GABA-A R mediated inhibitory function. Perforated-patch clamp recordings with the compound antibiotic gramicidin provide electrical access to the cell through the formation of pores in the membrane, permeable to cations but impermeant to Cl^-. Perforated-patch recordings with gramicidin have been successfully used in vitro to record GABAergic synaptic currents, while keeping intracellular Cl^- unaffected by the pipette solution[10, 11, 16, 21]. But previous work has also demonstrated that Cl^- gradient can be affected by the slicing procedure [22, 23], questioning the claims for excitatory GABAergic transmission based on in vitro recordings [23].

In vivo treatment with the diuretic bumetanide, which also reduces the accumulation of Cl^- ions in neurons through the inhibition of the Cl^- intruder NKCC1, was found to reduce behavioural abnormalities in rat and mouse models of Autism Spectrum Disorders[5] and seizures in animal models of epilepsy [24-28]. But bumetanide has a limited bio-availability in the brain due to poor blood brain barrier penetration[29-31], and it is finally unclear if its action in vivo was indeed due to the restoration of neuronal Cl^- gradient and inhibitory GABAergic transmission.

Direct investigation of the polarity of GABAergic transmission in vivo puts serious constraints in terms of experimental access, and the evaluation of synaptic responses to GABA-A R activation is challenging. Adapting to in vivo conditions the extracellular recording of unitary GABAergic postsynaptic potentials (field IPSPs) previously described in vitro[32-34], we could evaluate the polarity of perisomatic GABAergic signaling in the intact brain. As an exemple application, we now report the first direct evidence for depolarizing actions of perisomatic GABAergic transmission and time-locked excitation of CA3 pyramidal neurons in acute and chronic mouse models of epilepsy. We believe that this demonstration will pave the way for the investigation of Cl^- homeostasis and inhibitory function in

vivo, in physiological conditions and in situations in which alteration or even reversal of GABAergic transmission is hypothesized to occur. It also constitutes an invaluable tool to quantify the actual in vivo efficacy of drugs designed to modulate Cl^- homeostasis and restore physiological GABAergic inhibition, thereby meeting high clinical and therapeutical expectations.

Results

Extracellular recording of perisomatic field-IPSPs and time-locked inhibition of CA3 pyramidal cell firing in vivo.

Non-invasive recording of the dynamics of GABAergic synaptic transmission in vivo is a challenge. Previous work in vitro has suggested that perisomatic inhibitory postsynaptic signals originating from individual interneurons (basket and chandelier cells) could be recorded as extracellular field potentials (fIPSPs) from their target pyramidal-cell population[32-34]. This approach offers several main advantages. First, extracellular recordings preserve native $[Cl^-]i$. Second, the polarity of the field events indicates the direction of the current elicited in the target population of pyramidal cells, thereby addressing the question of depolarizing vs hyperpolarizing polarity of GABAergic postsynaptic signaling. And third, combined with units recording and spike sorting of neuronal discharges, extracellular detection of population fIPSPs provides a time reference to investigate the net effect of GABAergic perisomatic synaptic signals on the firing of the target neurons with single cell resolution, allowing a direct quantification of the efficacy of inhibition or excitation provided by perisomatic GABAergic inputs.

In order to evaluate the efficiency and polarity of perisomatic GABAergic transmission in the hippocampus in vivo, we have therefore inserted silicon probes into the dorsal CA3 pyramidal layer of urethane-anesthetized mice, recording spontaneous local field potentials and unitary neuronal activity. As illustrated in Fig. 1, spontaneous activity from the CA3 pyramidal layer included action potentials (units) and positive local field events with a profile similar to that of fIPSPs previously described in vitro as the GABA-A receptor mediated postsynaptic potentials originating from PV interneurons[34]. Accordingly, these events were characterized by a fast rise time (2.01±0.53ms, n=8 mice) and a decay time constant increased by the GABA-A modulator diazepam (2mg/kg, IP) from 3.65±0.05ms to 4.19±0.06ms (n=3 mice, $p<0.01$, two-tailed paired t-test, $t = 9.13$, $DF = 2$). As observed in vitro and expected from perisomatically projecting interneurons (basket and chandelier cells), in vivo fIPSPs provided very powerful time-locked inhibition of local pyramidal cells. Accordingly, multi-unit pyramidal cell activity was almost fully interrupted by fIPSPs, as observed in the traces shown in Fig. 1b and in the trough that follows fIPSPs in the peri-event time histogram (PETH) shown in Fig. 1d-e. Beside the peak firing that precedes fIPSPs and probably reflects the recruitment of perisomatic inhibition by pyramidal cells discharge[34], 79.05±14.93% of the 139 putative pyramidal cells obtained

from 8 mice were significantly inhibited by fIPSPs, resulting in a population firing reduced by 92.3±4.5%, returning to baseline values after 9.75±2.8ms (n=8 mice).

Perisomatic fIPSPs specifically originate from PV interneurons and provide homeostatic redistribution of individual pyramidal cells firing rates in the CA3 hippocampal network.

In order to verify that fIPSPs actually originate from PV interneurons, we recorded the extracellular field-potential responses to the optogenetic activation of PV interneurons. PV-Cre mice were injected with the DIO hChR2 (E123T/T159C)-EYFP construct in the CA3 region in order to express the cationic actuator ChR2 specifically in PV interneurons. PV immuno-staining of the infected mice showed excellent specificity, with 96 to 100% (98.3±2%, n=3 mice) of the infected (GFP-positive) cells being also PV-positive (Supplementary Fig. 1a). As illustrated in Fig. 2, brief (2ms) local optogenetic activation of PV interneurons did evoke reliable fIPSPs, together with powerfull time-locked inhibition of local pyramidal cells (n=33 pyramidal cells from 5 mice). PV interneuron firing is therefore sufficient to evoke fIPSPs. In order to know whether other types of interneurons also significantly contributed to the generation of perisomatic fIPSPs during spontaneous CA3 activity, PV-Cre mice were injected with the FLEX-rev::PSAML141F,Y115F:GlyR-IRES-GFP construct to express the inhibitory pharmacogenetic actuator PSAM-GlyR specifically in PV interneurons. PV immuno-staining of the infected mice showed that in addition to high specifity (99±1%, n=3 mice), 98±1 % (n=3 mice) of the PV-positive cells in the region of recording were also GFP-positive (Supplementary Fig. 1b), indicating that most PV interneurons expressed PSAM-GlyR. As illustrated in Fig. 3g-h, the pharmacogenetic inhibition of PV interneurons induced by local injection of the exogenous ligand PSEM-89S very efficiently suppressed spontaneous fIPSPs, from 6.58±3.50 to 0.45±0.66 events/s (n= 5 mice, $p<0.05$, two-sided Wilcoxon Mann-Whitney Test), suggesting that the recorded fIPSPs originated predominantly from PV interneurons.

Even though pharmacogenetic silencing of PV interneurons in the anesthetized mouse did not increase the global firing rate of the CA3 pyramidal cell population (Fig. 3h, 1.19±2.72Hz in control vs 0.96±1.04Hz in PSEM-89S, n=5 mice, NS, two-sided Wilcoxon Mann-Whitney Test), it did affect individual cells firing. As illustrated in Supplementary Fig. 2, the correlation coefficient between individual cells firing rates in consecutive epochs of 10min indicated a remarkable stability, both in baseline ($r=0.987$, $p<0.001$) and after PV interneuron silencing ($r=0.79$, $p<0.001$). On the other hand, as illustrated in Fig. 3i, the firing rates before vs after PSEM-89S were hardly correlated ($r=0.38$, $p<0.05$), indicating that PV interneuron silencing induced a redistribution of firing rates among pyramidal neurons within the CA3 circuit.

Depolarizing and excitatory perisomatic GABAergic transmission in acute seizures in the drug-free mouse.

The reversal potential of Cl-mediated GABAergic currents (E-GABA) is controlled by the passive movement and active transport of Cl- through various ionic channels and transporters in the plasma membrane. During spontaneous activity, Cl^- ions flowing through GABA-A channels tend to shift the reversal potential of GABAergic currents toward membrane potential. E-GABA is therefore a very dynamic process that depends on ongoing fluctuations of membrane potential and GABAergic conductances. During seizures, GABA is massively released by interneurons while pyramidal cells are depolarized, therefore getting loaded with Cl^- until extrusion mechanisms restore an hyperpolarizing Cl^- gradient. It is therefore expected that due to the time course of Cl^- extrusion, high Cl^- load and excitatory GABA might participate in a deficit of inhibition immediately after a seizure[16, 35]. However, the time dynamics of Cl^- balance through intrusion and extrusion systems that has been studied in vitro largely remains to be characterized in vivo. As illustrated in Fig. 4, taking advantage of fIPSPs as a non invasive index of the polarity of GABAergic currents in the CA3 pyramidal population, we have investigated the dynamics of perisomatic inhibition during acute interictal and ictal seizures in unanesthetized mice. In order to monitor both spontaneous and evoked fPISPs, PV-Cre mice were infected with the DIO-hChR2-EYFP construct in the CA3 region. Light stimulation with a locally positioned optical fiber provided evoked fIPSPs by direct stimulation of PV interneurons. Acute seizures were induced by a brief and focal intra-hippocampal injection of the convulsive agent bicuculline in the contralateral hemisphere. Electrophysiological recordings displayed both interictal activity and hippocampal ictal seizures, recognized as complex events lasting 30 to 40 seconds (39.25 ±2.5s, n=6 seizures from 4 mice), even though the animal did not show behavioural convulsions. While in comparison to baseline, fIPSPs were not significantly affected between epileptic discharges, they transiently appeared with a reversed polarity after the termination of ictal seizures, returning to normal polarity within 182 to 434 seconds after the termination of the seizure event (219.76±128.56s, n=6 seizures from 4 mice), suggesting transiently reversed polarity of GABAergic transmission after ictal seizures, but not after acute interictal discharges. Moreover, reversed fIPSPs entrained the discharge of postsynaptic neurons, as indicated by the peak in the peri-event histograms between reversed fIPSPs and multi-unit activity, suggesting not only depolarizing but also excitatory action of perisomatic GABAergic synaptic transmission. No more fIPSP-related excitatory interactions were seen after the recovery of the polarity of fIPSPs. These results suggest that an ictal seizure can entrain transient depolarizing and excitatory actions of perisomatic GABAergic transmission in the CA3 circuit.

Discrete excitatory perisomatic GABAergic transmission in a chronic model of epilepsy.

Acute ictal seizures, as induced experimentally by the injection of the convulsive agent kainic acid (KA), can turn into chronic epilepsy after a silent period of up to several weeks. Previous work on another model of epilepsy has suggested that reversed (excitatory) GABAergic transmission might be involved in the transition between acute seizures and chronic epilepsy[11, 14, 27]. This condition is of high clinical relevance because incident occurrence of isolated seizures in human is known to be a main factor for the development of chronic epilepsy after a latent period that can last from months to several years[36]. Identifying the cellular mechanisms responsible for this transition would therefore potentially offer opportunities for preventive treatment against epilepsy.

We have evaluated the dynamics of perisomatic inhibition in the CA3 hippocampal region of anesthetized KA-treated mice during the latent period, one week after KA injection in the contralateral hippocampus[37]. Interictal discharges were present in all KA-treated mice, but in none of the control animals (Supplementary Fig. 3). Among all identified fIPSPs, none appeared of reversed polarity, whether in control or in KA-treated mice, suggesting that GABAergic transmission remained globally hyperpolarizing at the network level. Nevertheless, because the polarity of fIPSPs represents the average response of all the local pyramidal targets of the discharging presynaptic interneuron(s), the possibility remained that a subpopulation of pyramidal cells might be depolarized or even excited by GABAergic transmission in spite of a globally hyperpolarizing fIPSP population response. We therefore evaluated the response of individual neurons to spontaneous fIPSPs, and indeed identified a minority of neurons (n=4 out of 78 putative pyramidal cells from 3 KA-treated mice, among a total of 195 putative pyramidal cells from 8 KA-treated mice) that fired action potentials in response to GABAergic synaptic inputs. Individual examples of putative pyramidal cells displaying the three distinct types of observed responses to spontaneous fIPSPs (time locked excitation, time-locked inhibition, or no clear change in net firing rate) are illustrated in Fig. 5. Therefore, analyzing single cell responses to fIPSPs revealed an heterogenity of GABAergic alterations among KA-injected animals. These observations suggest that fIPSPs in vivo may be useful to investigate whether the extent of reversed GABAergic transmission at various delays after an acute seizure episode is involved in the distinct etiological outcome among individual animals, differentially affected by the initial insult.

Discussion

The possibility that altered Cl^- homeostasis and functionally reversed GABAergic transmission (from inhibitory to excitatory) might be involved in major pathologies such as epilepsy, autism spectrum disorders or schizophrenia, has recently raised considerable interest[2-5, 10-15, 18, 19, 25, 26, 38, 39]. However, a direct assessment of this hypothesis has been hindered by the technical difficulty of

probing Cl^- gradient and GABAergic synaptic function in vivo. Neuronal $[Cl^-]i$ is very labile and even intracellular recordings with sharp electrodes, which limit cytoplasmic wash-out, do not preserve membrane integrity, potentially altering resting potential and endogenous Cl^- gradient. Indirect evaluation of pyramidal cell response to optogenetic activation of GABAergic interneurons from the frequency of glutamatergic inputs[23], or direct cell-attached recording of single-channel currents, including those evoked by GABA uncaging within the recording pipette[40], are elegant approaches but do not resolve the dynamics of synaptic transmission. On the other hand, previous work in vitro suggested that the postsynaptic response of hippocampal pyramidal cells to their perisomatic GABAergic inputs could be recorded extracellularly, as field-Inhibitory Postsynaptic Potentials (fIPSPs), and that the polarity of fIPSPs could be used as an index of Cl^- gradient and polarity of GABAergic transmission. Indeed, perisomatically projecting interneurons (basket and chandelier cells) have a densely arborised axon specifically confined to the pyramidal cell layer, and contact a large proportion of pyramidal cells within a restricted projection area[41, 42], so that each action potential of the interneuron triggers the nearly synchronous release of GABA on hundreds of target pyramidal cells, which postsynaptic responses (IPSPs) sum up and can be readily identified from a local extracellular electrode[32-34], with a polarity reflecting that of the Cl^- gradient[32, 33]. This approach is well suited to preserving endogenous $[Cl^-]i$, can be performed in vivo, and opens the possibility to resolve the dynamics of Cl^- gradient and polarity of GABAergic transmission over the course of ongoing synaptic activity. A strong limitation however is that fIPSPs are the average response of multiple pyramidal cells and therefore lack the resolution of individual cells, so that changes in GABAergic polarity could be detected if they affect the whole neuronal population but may be missed if affecting only a subset of cells. Morevover, GABAergic transmission involves both voltage and conductance changes, so that reversed $[Cl^-]i$ and depolarizing GABA carry a complex combination of excitatory (through depolarization) and inhibitory (through increased conductance) influences[21, 43-46]. As a consequence, determining the net postsynaptic effect of GABAergic transmission requires a direct readout of postsynaptic firing activity. For all these reasons, we now propose that the method of choice to probe Cl^- gradient and GABAergic synaptic function in vivo lies in combined multi-electrode recording and spike-sorting methods. While fIPSPs provide the timing and global (average) polarity of perisomatic GABAergic synaptic events, the distributions (peri-event time histograms) of the spikes of individually identified neurons provide the net functional effect of GABAergic transmission, with single cell resolution.

In line with previous in vitro evidence for the direct involvement of basket and chandelier cells in the generation of fIPSPs[32-34], we provide direct evidence that in vivo fIPSPs originate mostly from PV interneurons, because they were elicited by the optogenetic activation of PV interneuronal firing, and largely eliminated by the pharmacogenetic inhibition of PV interneuronal firing. Perisomatic inhibition

is considered to be functionally optimal for the control of neuronal discharge, with synapses strategically located on the soma and close to the site of action potential initiation[47, 48]. PV basket and chandelier cells are thus considered to play a major role in the control of pyramidal cells firing through time-locked inhibition, presumably preventing excessive firing within the hippocampal circuit. However, in spite of the critical importance of excitatory-inhibitory interactions in the recurrent CA3 circuit, the literature is strikingly missing direct reports of the dynamics of excitatory-inhibitory interactions in this neuronal circuit, presumably because of the technical difficulties to identify perisomatic inhibitory events in vivo. Our experimental results confirm that perisomatic GABAergic transmission provides very powerful time-locked inhibition of most CA3 pyramidal neurons. An interesting observation is that the blockade of PV interneuron firing was responsible for a redistribution of pyramidal cell activity, but was not accompanied by any major quantitative change of activity at the network level. This suggests that perisomatic inhibition may be involved in the control of the timing of pyramidal cells discharge rather than quantitative control of the network discharge. Previous reports are compatible with this hypothesis. In a previous study conducted in vitro, we have reported that fIPSPs were rather poorly recruited by network activity, suggesting that perisomatic inhibition should be more efficient in shaping the timing of spike flow than in limiting excitatory runaway recruitment and preventing the generation of hyper-synchronized discharges. Previous report that transgenic mice with specifically disrupted glutamatergic inputs to parvalbumin-positive interneurons displayed hippocampo-dependent spatial memory impairment but no epileptic phenotype are also in support of this interpretation[49, 50].

But one major advantage offered by the extracellular recording of fIPSPs is the possibility to evaluate the efficiency, and even the polarity, of perisomatic GABAergic transmission in a variety of conditions, including pathological conditions in which GABAergic transmission is suspected to be affected, or even reversed, due to altered neuronal Cl^- homeostasis. Cl^- gradient is dependent on both recent neuronal activity involving Cl^- currents and the dynamics of pumps and transporters involved in maintaining physiological Cl^- gradient. Our experiments have tested the possibility to detect the consequences for Cl^- regulation and GABAergic transmission of both acute hyperactivity and chronic epilepsy. We report that transient hypersynchronized discharges induce a global reversal of neuronal Cl^- and polarity of GABAergic transmission, shifting from inhibitory to excitatory for a duration of several tens of seconds before returning to normal polarity and efficiency. While this reversal of GABAergic polarity is readily seen as a reversed polarity of fIPSPs, we also report a more subtle effect during the course of epileptogenesis in the KA model of chronic epilepsy. One week after KA injection, we observed that perisomatic GABAergic transmission provided time-locked excitation to a minority of pyramidal neurons in the hippocampus, while we did not observe a reversed polarity of fIPSPs. This suggests that subtle alterations in the regulation of Cl^- homeostasis and GABAergic transmission

already operate in the hippocampal circuit during the latent period that precedes the establishment of chronic epilepsy. The functional consequences of defective GABAergic transmission in a minority of neurons, both in terms of coding and circuit dynamics, remain to be investigated. Independently of seizure generation, reversed GABAergic transmission might significantly affect neuronal processing and information coding.

The extracellular detection of perisomatic IPSPs therefore provides an invaluable tool to evaluate Cl^- homeostasis and inhibitory function, in physiological conditions and in situations in which alteration or even reversal of GABAergic transmission is hypothesized to occur. This approach opens new possibilities to evaluate the relevance of the excitatory GABA hypothesis in physiological development, autism spectrum disorders, schizophrenia, various forms of epilepsy and the time course of epileptogenesis, as well as to evaluate the potential of pharmacological interference with neuronal Cl^- gradient as an effective therapeutic strategy against major brain diseases.

Acknowledgements. We thank Roustem Khazipov, Rosa Cossart, Valérie Crepel, Tarek Deeb and Isabel Del Pino for useful comments and discussions on a previous version of the manuscript, Delphine Gonzales, Nathalie Aubailly, and all the personnel of the Animal Facility of the NeuroCentre Magendie for animal care, Katy Lecorf for her help regarding virus preparation, the UMR5293 vector core facility for producing AAV vectors, and the laboratory of S.M. Sternson (Howard Hughes Medical Institute) for providing the chemical compound PSEM-89S.

Funding. This work was performed thanks to the following funding sources: INSERM, CNRS (XL), Région Nouvelle Aquitaine (XL, AB), the Japanese Society for the Promotion of Science (JSPS, XL, HH), the Brain and Behavior Research Foundation (AB), Agence Nationale pour la Recherche (ANR, XL), the Fondation Française pour la Recherche sur les Epilepsies (FFRE, XL), the French Ministry of Research and Education (OD). The funders had no role in study design, data collection and analysis, decision to publish, or preparation of the manuscript.

Competing interests. The authors have declared that no competing interests exist.

Author contributions. XL and HH performed pilot experiments and initiated the study. XL conceived and designed the experiments. OD and XL planned the study. OD, A. Ferreira, AB and XL performed the experiments. OD and XL analyzed the data. A. Frick contributed with lab and breeding space, and a fraction of running expenses. OD, AB and XL wrote the paper.

Data availability. The data shown in the paper will be made available upon reasonable request to the corresponding author.

Code availability. The custom code used for analysis will be made available upon reasonable request to the corresponding author.

References

1. Blaesse, P., Airaksinen, M.S., Rivera, C. & Kaila, K. Cation-Chloride Cotransporters and Neuronal Function. *Neuron* **61**, 820-838 (2009).
2. Ben-Ari, Y. NKCC1 Chloride Importer Antagonists Attenuate Many Neurological and Psychiatric Disorders. *Trends in Neurosciences* **40**, 536-554 (2017).
3. Doyon, N., Vinay, L., Prescott, Steven A. & De Koninck, Y. Chloride Regulation: A Dynamic Equilibrium Crucial for Synaptic Inhibition. *Neuron* **89**, 1157-1172 (2016).
4. Deidda, G., *et al.* Reversing excitatory GABAAR signaling restores synaptic plasticity and memory in a mouse model of Down syndrome. *Nature Medecine* **21**, 318-326 (2015).
5. Tyzio, R., *et al.* Oxytocin-mediated GABA inhibition during delivery attenuates autism pathogenesis in rodent offspring. *Science* **343**, 675-679 (2014).
6. Lopez-Pigozzi, D., *et al.* Altered Oscillatory Dynamics of CA1 Parvalbumin Basket Cells during Theta–Gamma Rhythmopathies of Temporal Lobe Epilepsy. *eNeuro* **3**, ENEURO.0284-0216.2016 (2016).
7. Valero, M., *et al.* Mechanisms for Selective Single-Cell Reactivation during Offline Sharp-Wave Ripples and Their Distortion by Fast Ripples. *Neuron* **94**, 1234-1247.e1237 (2017).
8. Menendez de la Prida, L. & Trevelyan, A.J. Cellular mechanisms of high frequency oscillations in epilepsy: On the diverse sources of pathological activities. *Epilepsy Research* **97**, 308-317 (2011).
9. Cellot, G. & Cherubini, E. GABAergic Signaling as Therapeutic Target for Autism Spectrum Disorders. *Frontiers in Pediatrics* **2** (2014).
10. Barmashenko, G., Hefft, S., Aertsen, A., Kirschstein, T. & Köhling, R. Positive shifts of the GABAA receptor reversal potential due to altered chloride homeostasis is widespread after status epilepticus. *Epilepsia* **52**, 1570-1578 (2011).
11. Pathak, H.R., *et al.* Disrupted Dentate Granule Cell Chloride Regulation Enhances Synaptic Excitability during Development of Temporal Lobe Epilepsy. *The Journal of Neuroscience* **27**, 14012-14022 (2007).
12. Nardou, R., *et al.* Neuronal chloride accumulation and excitatory GABA underlie aggravation of neonatal epileptiform activities by phenobarbital. *Brain* **134**, 987-1002 (2011).
13. Moore, Y.E., Kelley, M.R., Brandon, N.J., Deeb, T.Z. & Moss, S.J. Seizing Control of KCC2: A New Therapeutic Target for Epilepsy. *Trends in Neurosciences* **40**, 555-571 (2017).
14. Bragin, D.E., Sanderson, J.L., Peterson, S., Connor, J.A. & Müller, W.S. Development of epileptiform excitability in the deep entorhinal cortex after status epilepticus. *European Journal of Neuroscience* **30**, 611-624 (2009).
15. Chen, L., *et al.* KCC2 downregulation facilitates epileptic seizures. *Scientific Reports* **7**, 156 (2017).

16. Ellender, T.J., Raimondo, J.V., Irkle, A., Lamsa, K.P. & Akerman, C.J. Excitatory Effects of Parvalbumin-Expressing Interneurons Maintain Hippocampal Epileptiform Activity via Synchronous Afterdischarges. *The Journal of Neuroscience* **34**, 15208-15222 (2014).

17. Di Cristo, G., Awad, P.N., Hamidi, S. & Avoli, M. KCC2, epileptiform synchronization, and epileptic disorders. *Progress in Neurobiology* **162**, 1-16 (2018).

18. Cohen, I., Navarro, V., Clemenceau, S., Baulac, M. & Miles, R. On the Origin of Interictal Activity in Human Temporal Lobe Epilepsy in Vitro. *Science* **298**, 1418-1421 (2002).

19. Huberfeld, G., *et al.* Perturbed Chloride Homeostasis and GABAergic Signaling in Human Temporal Lobe Epilepsy. *The Journal of Neuroscience* **27**, 9866-9873 (2007).

20. Pallud, J., *et al.* Cortical GABAergic excitation contributes to epileptic activities around human glioma. *Science Translational Medicine* **6**, 244ra289-244ra289 (2014).

21. Gulledge, A.T. & Stuart, G.J. Excitatory actions of GABA in the cortex. *Neuron* **37**, 299-309 (2003).

22. van der Pol, A.N., Obrietan, K. & Chen, G. Excitatory Actions of GABA after Neuronal Trauma. *The Journal of Neuroscience* **16**, 4283-4292 (1996).

23. Valeeva, G., Tressard, T., Mukhtarov, M., Baude, A. & Khazipov, R. An Optogenetic Approach for Investigation of Excitatory and Inhibitory Network GABA Actions in Mice Expressing Channelrhodopsin-2 in GABAergic Neurons. *The Journal of Neuroscience* **36**, 5961-5973 (2016).

24. Dzhala, V.I., *et al.* NKCC1 transporter facilitates seizures in the developing brain. *Nature Medicine* **11**, 1205 (2005).

25. Kahle, K.T. & Staley, K.J. The bumetanide-sensitive Na-K-2Cl cotransporter NKCC1 as a potential target of a novel mechanism-based treatment strategy for neonatal seizures. *Neurosurgical Focus* **25**, E22 (2008).

26. Marguet, S.L., *et al.* Treatment during a vulnerable developmental period rescues a genetic epilepsy. *Nature Medecine* **21**, 1436-1444 (2015).

27. Kourdougli, N., *et al.* Depolarizing γ-aminobutyric acid contributes to glutamatergic network rewiring in epilepsy. *Annals of Neurology* **81**, 251-265 (2017).

28. Brandt, C., Nozadze, M., Heuchert, N., Rattka, M. & Löscher, W. Disease-Modifying Effects of Phenobarbital and the NKCC1 Inhibitor Bumetanide in the Pilocarpine Model of Temporal Lobe Epilepsy. *The Journal of Neuroscience* **30**, 8602-8612 (2010).

29. Römermann, K., *et al.* Multiple blood-brain barrier transport mechanisms limit bumetanide accumulation, and therapeutic potential, in the mammalian brain. *Neuropharmacology* **117**, 182-194 (2017).

30. Donovan, M.D., Schellekens, H., Boylan, G.B., Cryan, J.F. & Griffin, B.T. In vitro bidirectional permeability studies identify pharmacokinetic limitations of NKCC1 inhibitor bumetanide. *European Journal of Pharmacology* **770**, 117-125 (2016).

31. Puskarjov, M., Kahle, K.T., Ruusuvuori, E. & Kaila, K. Pharmacotherapeutic targeting of cation-chloride cotransporters in neonatal seizures. *Epilepsia* **55**, 806-818 (2014).

32. Glickfeld, L.L., Roberts, J.D., Somogyi, P. & Scanziani, M. Interneurons hyperpolarize pyramidal cells along their entire somatodendritic axis. *Nature Neuroscience* **12**, 21-23 (2009).

33. Bazelot, M., Dinocourt, C., Cohen, I. & Miles, R. Unitary inhibitory field potentials in the CA3 region of rat hippocampus. *J Physiol* **588**, 2077-2090 (2010).

34. Beyeler, A., *et al.* Recruitment of Perisomatic Inhibition during Spontaneous Hippocampal Activity. *PLoS.One.* **8**, e66509 (2013).

35. Fujiwara-Tsukamoto, Y., Isomura, Y., Nambu, A. & Takada, M. Excitatory GABA input directly drives seizure-like rhythmic synchronization in mature hippocampal CA1 pyramidal cells. *Neuroscience* **119**, 265-275 (2003).

36. French, J.A., *et al.* Characteristics of medial temporal lobe epilepsy: I. Results of history and physical examination. *Annals of Neurology* **34**, 774-780 (1993).

37. Riban, V., *et al.* Evolution of hippocampal epileptic activity during the development of hippocampal sclerosis in a mouse model of temporal lobe epilepsy. *Neuroscience* **112**, 101-111 (2002).

38. Löscher, W., Puskarjov, M. & Kaila, K. Cation-chloride cotransporters NKCC1 and KCC2 as potential targets for novel antiepileptic and antiepileptogenic treatments. *Neuropharmacology* **69**, 62-74 (2013).

39. MacKenzie, G., O'Toole, K.K., Moss, S.J. & Maguire, J. Compromised GABAergic inhibition contributes to tumor-associated epilepsy. *Epilepsy Research* **126**, 185-196 (2016).

40. Minlebaev, M., Valeeva, G., Tcheremiskine, V., Coustillier, G. & Khazipov, R. Cell-attached recordings of responses evoked by photorelease of GABA in the immature cortical neurons. *Frontiers in Cellular Neuroscience* **7** (2013).

41. Sik, A., Penttonen, M., Ylinen, A. & Buzsaki, G. Hippocampal CA1 interneurons: an in vivo intracellular labeling study. *The Journal of Neuroscience* **15**, 6651-6665 (1995).

42. Buhl, E.H., *et al.* Physiological properties of anatomically identified axo-axonic cells in the rat hippocampus. *Journal of Neurophysiology* **71**, 1289-1307 (1994).

43. Kirmse, K., *et al.* GABA depolarizes immature neurons and inhibits network activity in the neonatal neocortex in vivo. *Nature Communications* **6**, 7750 (2015).

44. Khalilov, I., Minlebaev, M., Mukhtarov, M. & Khazipov, R. Dynamic Changes from Depolarizing to Hyperpolarizing GABAergic Actions during Giant Depolarizing Potentials in the Neonatal Rat Hippocampus. *The Journal of Neuroscience* **35**, 12635-12642 (2015).

45. Staley, K.J. & Mody, I. Shunting of excitatory input to dentate gyrus granule cells by a depolarizing GABAA receptor-mediated postsynaptic conductance. *Journal of Neurophysiology* **68**, 197-212 (1992).

46. Tyzio, R., *et al.* Postnatal changes in somatic gamma-aminobutyric acid signalling in the rat hippocampus. *European Journal of Neuroscience* **27**, 2515-2528 (2008).

47. Somogyi, P. & Klausberger, T. Defined types of cortical interneurone structure space and spike timing in the hippocampus. *J Physiol* **562**, 9-26 (2005).

48. Miles, R., Toth, K., Gulyas, A.I., Hajos, N. & Freund, T.F. Differences between somatic and dendritic inhibition in the hippocampus. *Neuron* **16**, 815-823 (1996).

49. Racz, A., Ponomarenko, A.A., Fuchs, E.C. & Monyer, H. Augmented hippocampal ripple oscillations in mice with reduced fast excitation onto parvalbumin-positive cells. *The Journal of Neuroscience* **29**, 2563-2568 (2009).

50. Fuchs, E.C., *et al.* Recruitment of parvalbumin-positive interneurons determines hippocampal function and associated behavior. *Neuron* **53**, 591-604 (2007).

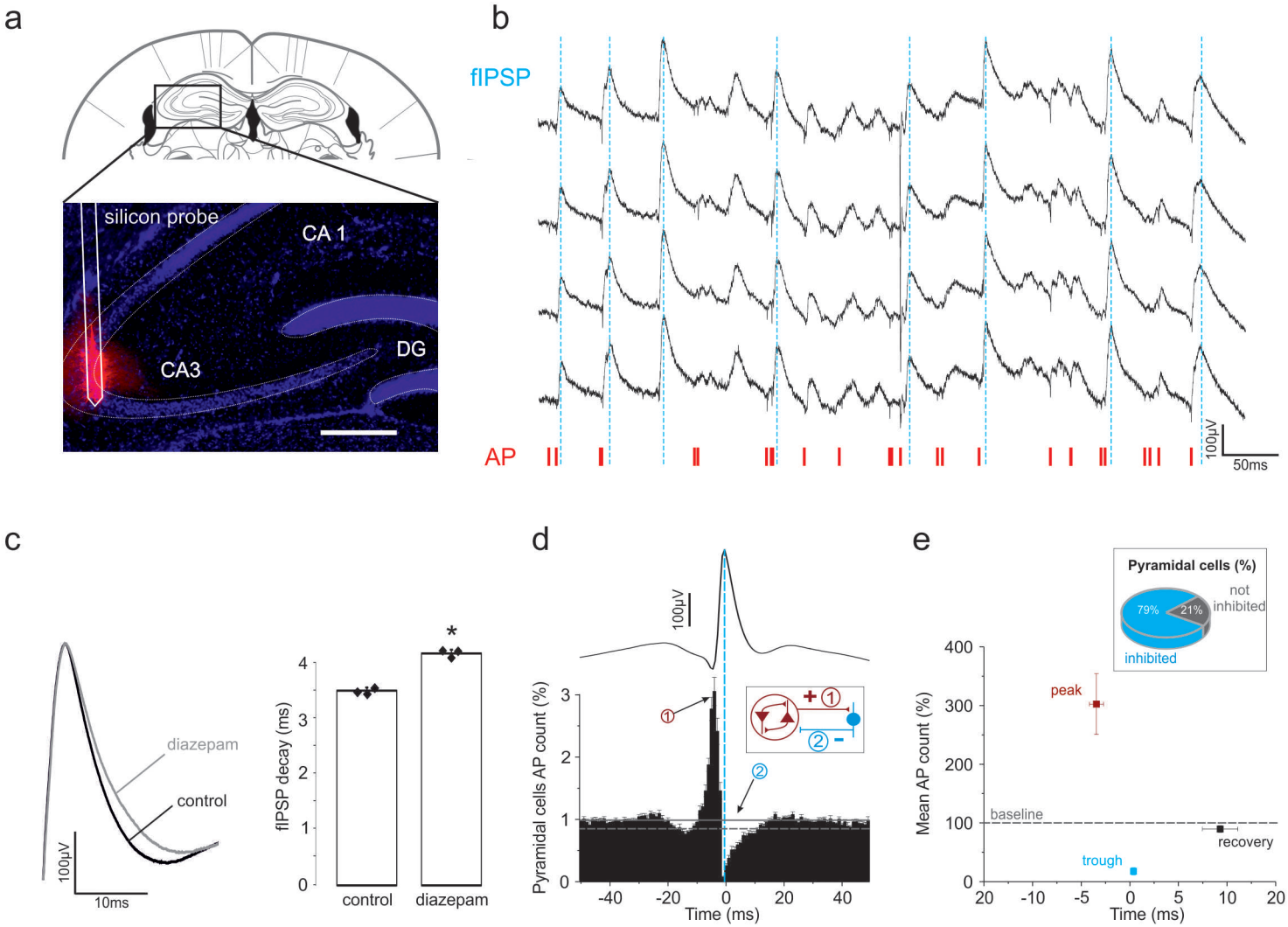

Figure 1: Spontaneous extracellular field inhibitory post-synaptic potentials (fIPSPs) in vivo

(a) Schematic of electrode track and histological verification of recording location within the CA3 hippocampal region (**DiI-labeled silicon probe in red**, **DAPI staining in blue**).

(b) Exemple trace of spontaneous wide-band (0.1Hz-9KHz) field-recording activity in the CA3 pyramidal layer, displaying 4 channels (10-20µm distance between recording sites) of the same shank of a 2-shanks Neuronexus Buzsaki16 silicon probe. Field-events of positive polarity (upward deflections), fIPSPs (peaks, **dashed blue lines)**. Fast downward deflections, action potentials (AP), also labeled below as raster display (**red ticks,** multi-unit activity). Note the transient interruption of neuronal firing after fIPSPs.

(c) Comparison of fIPSP decay (left, superimposed average traces normalized on amplitude, right, fIPSPs decay times, mean± SD, ** $p<0.01$) in control (**black**) and in presence of diazepam (**grey**). Note prolonged fIPSP decay under diazepam.

(d) Peri-event time histogram (mean and SD, n=8 WT mice, time bin 1 ms) between all the spikes discharged by putative pyramidal cells and fIPSPs (reference, peak-time), shown as average trace on top at the same time scale and aligned on peak (**dotted blue line**). Baseline mean and 2SD are respectively shown as **plain and dotted horizontal grey lines**. Note increased pyramidal cell discharge in the 10 ms prior to fIPSP, and the strong inhibition (trough, max inhibition) that follows. **Inset**, schematic illustration of the recurrent excitatory/inhibitory loop: **(1)** the collective discharge of interconnected pyramidal cells activates the discharge of local interneurons, resulting **(2)** in perisomatic fIPSP and inhibition of pyramidal population activity.

(e) Diagram illustrating firing rates (mean ± SD, same 8 mice as in D; baseline level = 100%, calculated from -50 ms to -30 ms) at **peak** (bin of maximum firing in the 10ms prior to fIPSPs), **trough** (bin of minimum firing in the 4ms post-fIPSPs), and **recovery** (last of post-fIPSPs time bin below baseline - 2SD) time points. **Inset**, proportion of pyramidal cells (n=139 from 8 mice) with a significant post-fIPSPs trough (ie inhibited vs not-inhibited neurons).

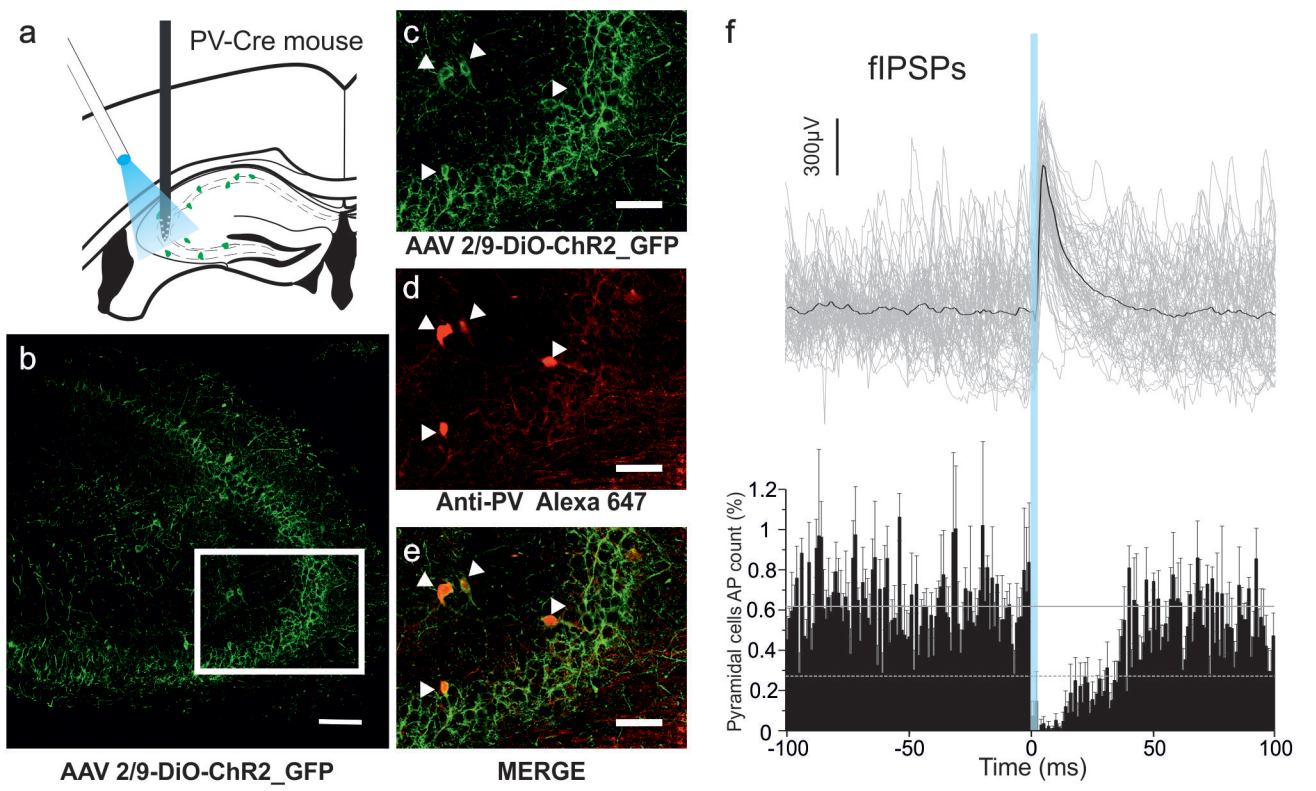

Figure 2: In vivo fIPSPs generated by optogenetic activation of PV interneurons
(a) Schematic representation of electrode and optic fiber positions in PV-Cre mice with AAV-driven ChR2 and GFP expression in CA3 PV interneurons.
(b-e) Confocal stacks of GFP-positive (**green**) and PV-positive (**red**) immunostaining in the hippocampal CA3 region. (**b**, **scale bar**, 100µm) GFP immuno staining. (**c-e**, **scale bar**, 50µm), higher magnification of the CA3a region delimited by the **white rectangle** in B). **(C)** GFP immuno-staining. **(d)** PV immunostaining. **(e)** Overlay. Note the co-localization on the 4 identified PV interneurons (arrow-heads).
(f) Peri-event time histogram (mean ± SD, n=5 mice, time bin 1 ms) between all the spikes discharged by putative pyramidal cells and optogenetically evoked (laser ON 2ms, **blue bar**) fIPSPs (reference), shown as superimposed (**grey**) and average (**black**) traces (n=60 from a single representative recording) on top, aligned and at the same time scale. Note the powerful time-locked inhibition of pyramidal cell firing in response to fIPSPs evoked by the optogenetic stimulation of PV interneurons.

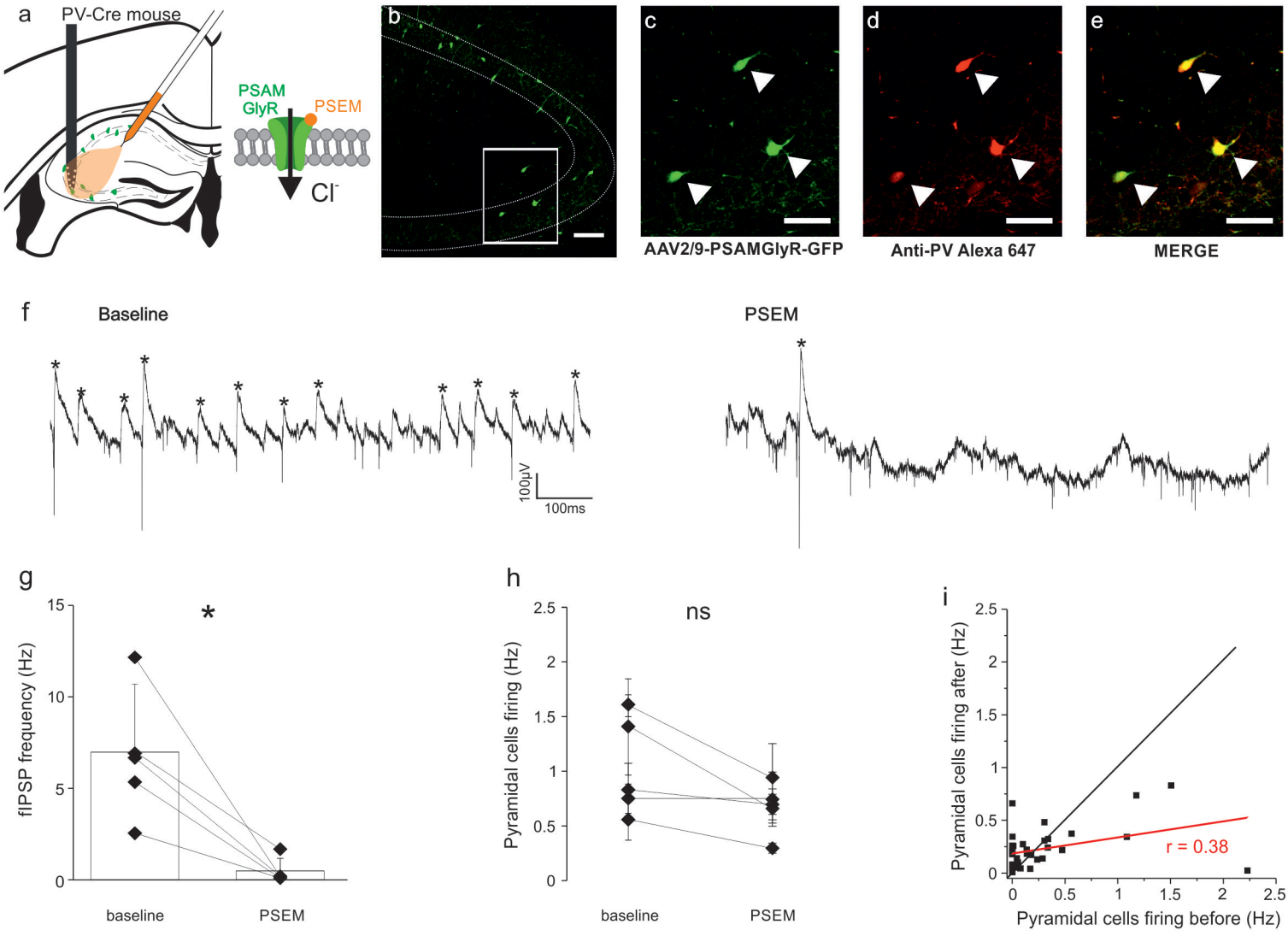

Figure 3: Inhibition of fIPSPs by pharmacogenetic inactivation of PV interneurons

(a) Schematic representation of electrode and injection site in PV-Cre mice with AAV-driven PSAM-GlyR and GFP expression in CA3 PV interneurons.

(b-e) Confocal stacks of GFP-positive (**green**) and PV-positive (**red**) immunostaining in the hippocampal CA3 region. (**b**, **scale bar**, 100µm) GFP immuno staining. (**c-e**, **scale bar**, 50µm), higher magnification of the CA3a region delimited by the **white rectangle** in B). **(c)** GFP immuno-staining. **(d)** PV immunostaining. **(e)** Overlay. Note the co-localization of PV and PSAM-GlyR immuno-staining on the 3 labeled interneurons (**arrow-heads**).

(f) Example traces of spontaneous wide-band (0.1Hz-9KHz) field-recording activity in the CA3 pyramidal layer, in control (left, **baseline**) and in presence of the exogenous ligand PSEM-89S (right, **PSEM**). Note the drastic reduction in fIPSPs expression (*).

(g-h) Summary plots (mean ± SD, n=5 mice) of fIPSP frequency **(g)** and pyramidal population firing rate **(h)** in control (baseline) and in presence of PSEM (* $p<0.05$).

(i) Individual pyramidal cells firing rates (n=36 putative pyramidal cells from 3 mice) in control ("**before**" is the 10min period that immediately preceeds PSEM-89S injection) and in presence of PSEM ("**after**" period is from 5 to 15min after PSEM-89S injection). **Black line**, bissector (y=x). **Red line**, linear regression line. Note that the pharmacogenetic blockade of PV interneurons with PSAM-GlyR redistributed individual firing rates without any significant change on global population firing activity.

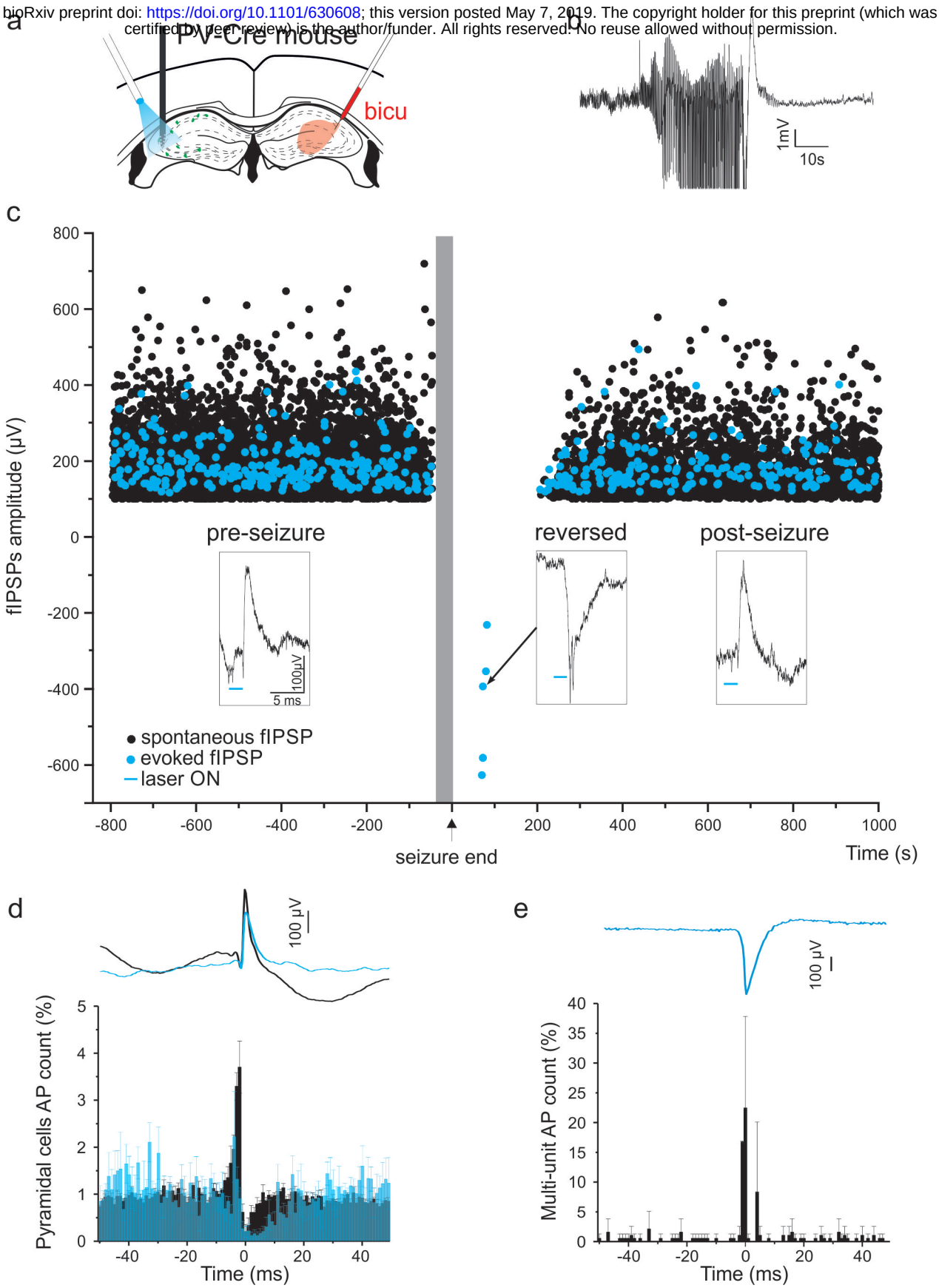

Figure 4: Transiently reversed fIPSPs and perisomatic GABAergic synaptic transmission following acute seizures

(a) Schematic representation of electrode and optic fiber positions in the left hippocampus of PV-Cre mice with AAV-driven ChR2 expression in CA3 PV interneurons, and contralateral injection of the convulsivant bicuculline.

(b) Exemple trace (wide-band LFP) of a seizure as acute response to contralateral bicuculline injection.

(c) Time course of individual fIPSPs amplitude (**black dots**, spontaneous, **blue dots**, evoked by optogenetic activation of PV interneurons), relative to acute seizures induced by the contralateral injection of bicuculline (**vertical grey bar**, 3 seizures from the same animal, aligned by their ending time). **Insets**, representative individual field responses (optogenetically evoked fIPSPs; **horizontal blue bars**, laser ON) in control (**pre-seizure**), during the period right after the seizure (**reversed polarity**), or after recovery (**post-seizure**). Note transiently evoked spiking activity induced by fIPSPs of reversed polarity right after the seizure and progressive recovery of fIPSPs amplitude.

(d) Peri-event time histogram (mean and SD, time bin 1ms) between all the spikes discharged by putative pyramidal cells (n=4 mice) and spontaneous (in **black**, n=31682 events) or optogenetically evoked (in **blue**, n=2756 events) fIPSPs (reference) from the pre- and post-seizure periods, shown as average traces on top (spontaneous, **black**; evoked, **blue**) at the same time scale and aligned on peak.

(e) Peri-event time histogram (mean and SD, time bin 1ms) between multi-unit activity and optogenetically evoked fIPSPs (reference) in the period right after the seizure (n=57 fIPSPs from 6 seizures from 4 mice), shown as average traces on top at the same time scale and aligned on peak. Note the clear time-locked excitation of neuronal firing and reversed polarity of the fIPSPs evoked by the optogenetic stimulation of PV interneurons in the period right after the seizure.

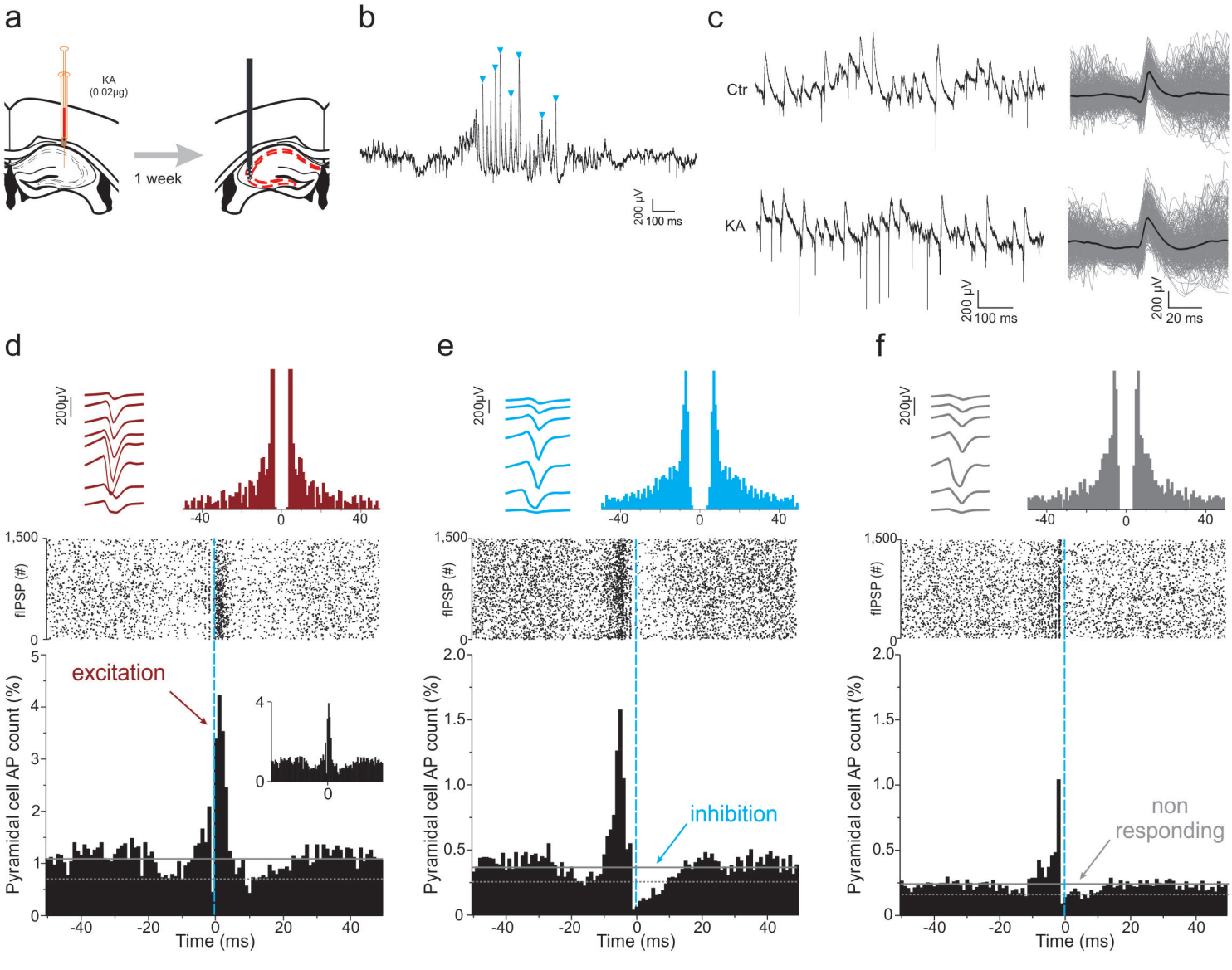

Figure 5: Normal fIPSP polarity but GABA-mediated time-locked excitation in head-fixed KA-treated mice
(a) CA3 neuronal activity was recorded from urethane-anesthetized WT mice one week after contralateral, intra-hippocampal KA injection.
(b) Exemple trace (wide-band LFP) of interictal burst (interictal spikes, **blue arrow-heads**).
(c) Exemple traces of spontaneous CA3 pyramidal layer activity (left) and superimposed and averaged traces of fIPSPs (right), in control (top) and KA (below) conditions. Note the presence of normal polarity, frequent fIPSPs, in both conditions.
(d-f) Individual examples of putative pyramidal cells displaying the three distinct types of observed responses to spontaneous fIPSPs in KA-treated mice (time locked excitation **(d)**, time-locked inhibition **(e)**, or no clear change in net firing rate (**f, non responding**)). **Upper left**, average waveform from the 8 channels of the recording electrode. **Upper right**, spike autocorrelogram. **Middle**, raster display of spike firing aligned on fIPSP ocurrence (**vertical blue line**, fIPSP peak). **Lower plot**, normalized peri-event time histogram (time bin, 1ms) of the neuron discharge (AP count) relative to fIPSP peak (reference, **vertical blue line**). **Inset (d)**, similar peri-event time histogram but ignoring action potential bursts (ie all spikes with preceding inter spike interval < 10ms omitted from the histogram).